Title

Sensing of bacterial type IV secretion via the unfolded protein response.

Journal

mBio, 4(1)

ISSN

2150-7511

Authors

de Jong, Maarten F
Starr, Tregei
Winter, Maria G
et al.

Publication Date

2013-02-01

DOI

10.1128/mbio.00418-12

Peer reviewed

Sensing of Bacterial Type IV Secretion via the Unfolded Protein Response

Maarten F. de Jong,[a,c] Tregei Starr,[b] Maria G. Winter,[a] Andreas B. den Hartigh,[a] Robert Child,[b] Leigh A. Knodler,[b]* Jan Maarten van Dijl,[c] Jean Celli,[b] Renée M. Tsolis[a]

Department of Medical Microbiology and Immunology, University of California, Davis, California, USA[a]; Laboratory of Intracellular Parasites, Rocky Mountain Laboratories, Hamilton, Montana, USA[b]; Department of Medical Microbiology, University of Groningen, University Medical Center Groningen, Groningen, The Netherlands[c]

* Present address: Leigh A. Knodler, Paul G. Allen School for Global Animal Health, Washington State University, Pullman, Washington, USA.

ABSTRACT **Host cytokine responses to *Brucella abortus* infection are elicited predominantly by the deployment of a type IV secretion system (T4SS). However, the mechanism by which the T4SS elicits inflammation remains unknown. Here we show that translocation of the T4SS substrate VceC into host cells induces proinflammatory responses. Ectopically expressed VceC interacted with the endoplasmic reticulum (ER) chaperone BiP/Grp78 and localized to the ER of HeLa cells. ER localization of VceC required a transmembrane domain in its N terminus. Notably, the expression of VceC resulted in reorganization of ER structures. In macrophages, VceC was required for *B. abortus*-induced inflammation by induction of the unfolded protein response by a process requiring inositol-requiring transmembrane kinase/endonuclease 1. Altogether, these findings suggest that translocation of the T4SS effector VceC induces ER stress, which results in the induction of proinflammatory host cell responses during *B. abortus* infection.**

IMPORTANCE ***Brucella* species are pathogens that require a type IV secretion system (T4SS) to survive in host cells and to maintain chronic infection. By as-yet-unknown pathways, the T4SS also elicits inflammatory responses in infected cells. Here we show that inflammation caused by the T4SS results in part from the sensing of a T4SS substrate, VceC, that localizes to the endoplasmic reticulum (ER), an intracellular site of *Brucella* replication. Possibly via binding of the ER chaperone BiP, VceC causes ER stress with concomitant expression of proinflammatory cytokines. Thus, induction of the unfolded protein response may represent a novel pathway by which host cells can detect pathogens deploying a T4SS.**

Received 4 October 2012 **Accepted** 16 January 2013 **Published** 19 February 2013

Citation de Jong MF, Starr T, Winter MG, den Hartigh AB, Child R, Knodler LA, van Dijl JM, Celli J, Tsolis RM. 2013. Sensing of bacterial type IV secretion via the unfolded protein response. mBio 4(1):e00418-12. doi: 10.1128/mBio.00418-12.

Invited Editor Craig Roy, Yale University School of Medicine

Editor Yasuko Rikihisa, Ohio State University

Address correspondence to Renee M. Tsolis, rmtsolis@ucdavis.edu.

Both commensals and nonpathogenic bacteria produce pathogen-associated molecular patterns (PAMPs) that stimulate innate immune responses in their eukaryotic hosts via pattern recognition receptors such as Toll-like receptors (TLRs). Importantly, virulence factors of pathogens provide additional signals that allow the innate immune system to differentiate between friend and foe (1). These factors include type III and IV secretion systems (T3SS and T4SS, respectively) that translocate bacterial PAMPs such as flagellin, peptidoglycan, or nucleic acids into the host cell cytosol, thereby activating cytosolic signaling pathways such as Nod-like receptors that induce proinflammatory cytokine expression via caspase-1 inflammasomes and activation of NF-κB (2, 3). In addition, both mammalian and plant hosts can sense interference by bacterial T3SS and T4SS effectors with critical signaling pathways such as signal transduction and translation by detecting "patterns of pathogenesis" (4–6).

The intracellular bacterial pathogen *Brucella abortus* is a good model for the identification of patterns of pathogenesis, because its PAMPs, such as lipopolysaccharide and flagellin, have very weak agonist activity for TLRs (7–9). The induction of inflammation by *B. abortus in vivo* is, for the most part, dependent on the activity of a T4SS. In a mouse infection model, this proinflammatory stimulus results in the induction of granulomatous inflammation and Th1 polarization of the immune response (10–12). However, the mechanism by which this response is elicited by the T4SS and the host cell pathways involved are unknown.

The T4SS of the human-pathogenic *Brucella* species (*B. abortus*, *B. suis*, and *B. melitensis*) is essential for persistent infection in cultured macrophages, in mice, and in goats, the latter being an important zoonotic reservoir host of *B. melitensis* (13–18). In macrophages, a primary target of *Brucella* during infection, expression of the T4SS-encoding *virB* operon is induced after acidification of the *Brucella*-containing vacuole (BCV) (19). The *Brucella* T4SS mediates the exclusion of phagolysosomal markers from the endosomal BCV and maturation to an endoplasmic reticulum (ER)-derived compartment (20–22). As a result, intracellular *B. abortus* can avoid degradation in phagolysosomes and, instead, this bacterium is found initially within vacuoles containing ER markers such as calreticulin (22). Later in infection, the bacteria localize to large, LAMP-1-positive vacuoles with features

of autophagosomes, named aBCVs (23). As *virB* mutant *Brucella* strains remain in lysosomal compartments and fail to replicate, it is thought that T4SS effectors may contribute to this subversion of the endocytic pathway.

Multiple reports have identified *Brucella* proteins whose translocation into the host cytosol is directly or indirectly dependent on the T4SS (13, 24, 25). One of these proteins, VceC, is translocated in a T4SS-dependent manner into macrophages during infection with *B. abortus*. However, its function and contribution to *Brucella* infection were so far unknown (13). In this study, we identified a host pathway involved in the sensing of VceC translocation into host cells, unveiling the first known intracellular activity for a T4SS substrate of *B. abortus*.

RESULTS

VceC is involved in induction of proinflammatory cytokines by the *B. abortus* T4SS. The VirB T4SS is involved in several aspects of host-pathogen interactions, including intracellular replication (16, 17), exclusion of LAMP-1, and targeting to the ER (20), and maintaining infection in both mice and goats (15, 18, 29). Furthermore, *in vivo*, the T4SS induces inflammatory responses early during infection (10, 12). To study the contribution of VceC to these T4SS-dependent phenotypes, a *B. abortus* mutant lacking the entire *vceC* gene (MDJ32) was constructed (see Fig. S1A in the supplemental material). The absence of *vceC* expression in MDJ32 was confirmed by Western blotting (see Fig. S1B). Notably, the *vceC* mutant (MDJ32) was able to survive and replicate inside both macrophages and HeLa cells to a level comparable to that of the wild-type *B. abortus* strain (see Fig. S1C and S2). Similar to wild-type *B. abortus*, the *vceC* mutant strain was able to exclude the late endosomal/lysosomal marker LAMP-1 and target to the ER, as evidenced by the colocalization of bacteria with calnexin at 24 h (see Fig. S2) (21). Also, the late targeting of *B. abortus* to aBCVs was unaffected at 72 h (see Fig. S2) (23). In the mouse infection model, strain MDJ32 (*vceC*) colonized mice initially at wild-type levels. However, at 4 and 8 weeks postinfection (p.i.), a small (50%) but statistically significant competitive defect in splenic colonization by MDJ32 (*vceC*) was observed (see Fig. S1D). These observations suggest that even though VceC is dispensable for persistence, it does enhance persistent colonization of the spleen in the mouse infection model.

In addition to survival in macrophages, the T4SS of *B. abortus* and *B. melitensis* was previously found to be required for the induction of genes encoding cytokines and chemokines in the spleens of infected mice (12). It can therefore be hypothesized that induction of the host's innate immune system by the *Brucella* T4SS is triggered directly, through the recognition of one or more of its effectors by host cells. To test whether VceC contributes to the T4SS-induced inflammation phenotype, we infected mouse bone marrow-derived macrophages (BMDM) with the *B. abortus* wild-type strain (2308); the T4SS-deficient *virB2* strain (ADH3), which lacks a predicted pilus protein; the *vceC* mutant strain (MDJ32); or a complemented *vceC* mutant. The results showed that wild-type *B. abortus* induces the secretion of proinflammatory cytokines interleukin-6 (IL-6) and tumor necrosis factor alpha (TNF-α), whereas relatively low levels of these cytokines were detected in the supernatants of uninfected macrophages (Fig. 1A and C). Compared to the wild-type strain, the *B. abortus virB2* mutant strain induced lower levels of cytokines, consistent with the observed *in vivo* proinflammatory role of the *Brucella* T4SS.

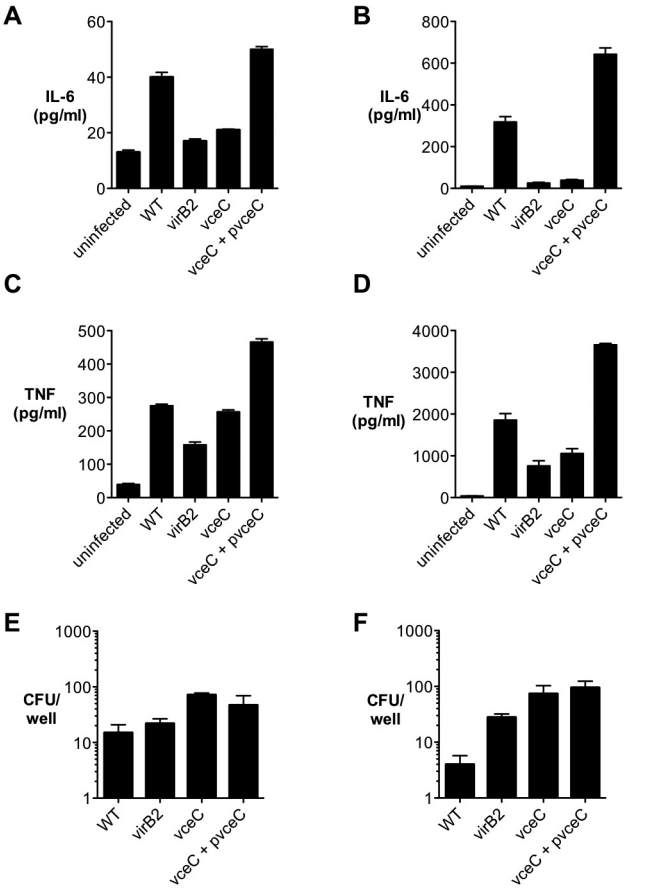

FIG 1 VceC is required for *B. abortus*-induced secretion of IL-6 and TNF-α (A to D). BMDM were infected for 24 h with wild-type (WT) *B. abortus* (2308), the *virB2* mutant (ADH3), the *vceC* mutant (MDJ32), or the complemented *vceC* mutant (MDJ71). Macrophages were either left untreated (A, C) or treated with 1 ng/ml IFN-γ (B, D) during infection. Levels of IL-6 (A, B) or TNF-α (C, D) in the macrophage supernatants were measured by ELISA. Data are expressed as means ± standard deviations and represent the results of a single experiment that was replicated three times independently with similar results. (E and F) Intracellular numbers of *B. abortus* CFU in BMDM with (E) and without (F) IFN-γ treatment.

Interestingly, infection of the macrophages with the *vceC* mutant also induced lower secretion of IL-6 and TNF-α than did wild-type *B. abortus* and this defect was restored by complementation of the *vceC* mutant strain with a plasmid-borne copy of *vceC* (Fig. 1A to D). Since production of gamma interferon (IFN-γ) by CD4 T cells is essential for control of *B. abortus* infection *in vivo* (30), we also determined whether VceC has the same activity in IFN-γ-activated macrophages (Fig. 1B and D). In IFN-γ-activated BMDM, we observed a more marked difference in IL-6 and TNF-α production by cells infected with wild-type *B. abortus* or the complemented *vceC* mutant than in those infected with the *vceC* mutant (Fig. 1B and D). These differences were not the result of differences in bacterial numbers, since compared to wild-type *B. abortus*, equal or higher numbers of mutant bacteria were present in the cells at 24 h p.i. (Fig. 1E and F). The VceC-dependent induction of TNF-α and IL-6 in infected macrophages suggests that VceC is sensed by an innate immune pathway in the cell that leads to downstream activation of NF-κB.

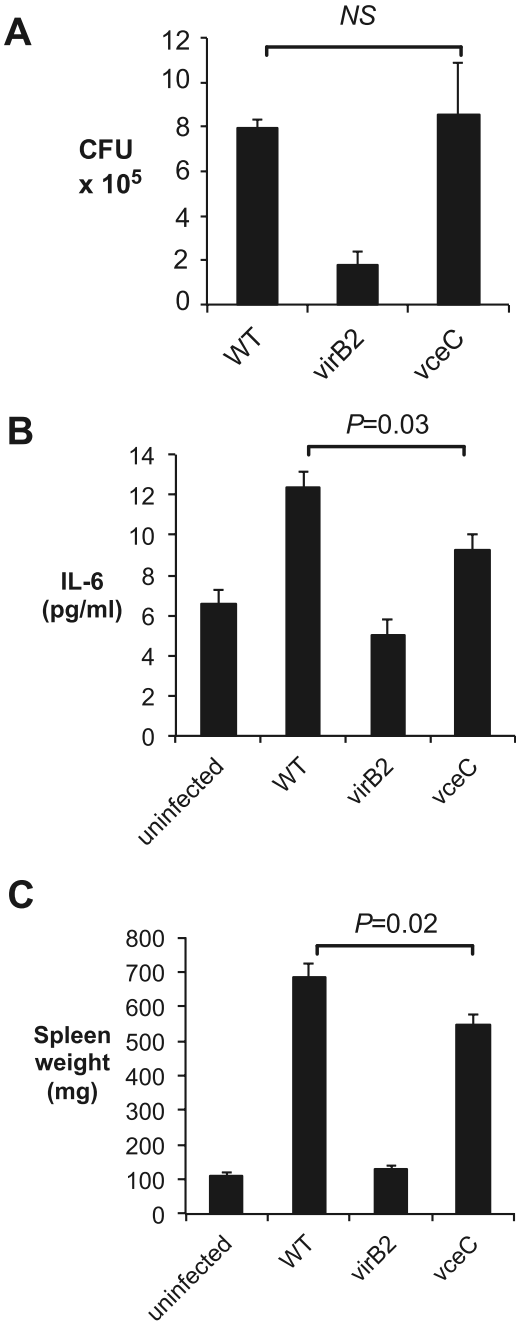

FIG 2 Groups of four C57BL/6 mice were infected with wild-type (WT) *B. abortus* (2308), the *virB2* mutant ADH3, or the *vceC* mutant MDJ32 and euthanized at day 14. (A) Total bacterial loads in mouse spleens. (B) Levels of circulating IL-6 measured by ELISA. (C) Spleen weights of infected mice. Data are expressed as means ± standard deviations, and the significance of differences was analyzed with a two-tailed Student *t* test.

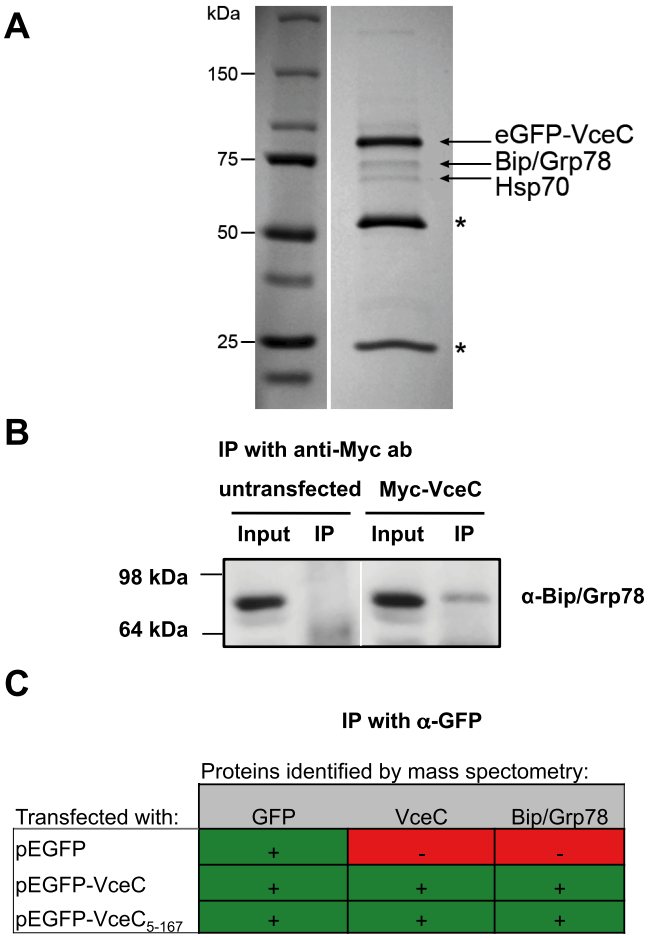

FIG 3 Interaction of VceC with the host ER chaperone BiP. (A) IP with anti-GFP antibodies was performed with HeLa cells expressing GFP-VceC, and the resulting IP fractions were resolved by SDS-PAGE and silver stained. Bands of 70 and 78 kDa, visible in the IP fraction of GFP-VceC were excised from the gel and subjected to LC-MS analysis. Asterisks indicate bands corresponding to the heavy and light chains of immunoglobulin. (B) Western blot probed with anti-BiP antibody showing the presence of BiP in the IP fraction of Myc-VceC-transfected cells but not in the IP fraction of untransfected cells. IP was performed with an antibody against the Myc tag. (C) Proteins identified by LC-MS in the IP fraction of GFP-, GFP-VceC-, or GFP-VceC$_{5-167}$-transfected HeLa cells. α-GFP, anti-GFP antibody.

To confirm the *in vitro* role of VceC in the induction of inflammation in an *in vivo* model, C57BL/6 mice were either mock infected or infected with the *B. abortus* wild-type, *virB2* mutant (ADH3), or *vceC* mutant (MDJ32) strain. As controls, a group of mice was mock infected. Inflammatory changes were evaluated at 14 days p.i. (Fig. 2). The *virB2* mutant was present in the spleen in reduced numbers compared to wild-type *B. abortus*, as demonstrated previously (31), while the *vceC* mutant colonized the spleen in numbers equal to those of the wild type (Fig. 2A). However, at this time point, circulating IL-6 levels were significantly lower in *vceC* mutant-infected mice than in mice infected with the wild-type strain ($P = 0.03$; Fig. 2B). Furthermore, a second measure of inflammatory changes, namely, spleen weight, was significantly reduced in mice infected with the *vceC* mutant ($P = 0.02$; Fig. 2C). This result suggests that T4SS-mediated translocation of VceC contributes to inflammation during the infection of mice by *B. abortus*.

VceC interacts with the ER chaperone BiP. To identify potential interaction partners of VceC that could contribute to its proinflammatory activity, we performed immunoprecipitation (IP) with HeLa cells expressing the enhanced-GFP (eGFP)-VceC or Myc-VceC fusion. In Fig. 3A, the IP fraction from cells expressing eGFP-VceC was resolved by SDS-PAGE, revealing two additional

bands of 70 and 78 kDa. Both the 70- and 78-kDa bands were subjected to LC-MS analysis (Fig. 3A). While the 70-kDa band was found to be Hsp70, a cytosolic chaperone, the 78-kDa band was identified as BiP/Grp78. BiP is a chaperone found in the lumen of the ER, where it plays a key role in protein secretion and in the maintenance of ER homeostasis (32–35). Of these two bands, only the BiP/Grp78 band was specific for VceC, while Hsp70 was pulled down in cells transfected with both eGFP-VceC and eGFP-VceA (a second *B. abortus* T4SS substrate, not shown in Fig. 3) and therefore was not analyzed further as a specific interaction partner of VceC.

To determine whether the interaction of GFP-VceC with BiP was related to the relatively large GFP moiety, the IP experiment was repeated with HeLa cells transiently transfected with a construct encoding VceC fused to the smaller Myc tag (Myc-VceC; Fig. 3B). Western blotting demonstrated the presence of BiP in the IP fraction of Myc-VceC-transfected HeLa cells but not in the IP fraction of untransfected cells.

VceC contains a central proline-rich region in which proline accounts for 25% of the amino acid residues. Since proline-rich domains have been implicated in protein-protein interactions of both bacterial and host factors (36–38), we also tested whether the proline-rich region of VceC is required for binding to BiP by repeating the IP experiments with HeLa cells expressing eGFP, eGFP-VceC, or eGFP-VceC$_{5\text{-}167}$, lacking the proline-rich region of VceC. As expected, LC-MS analysis identified peptides matching the GFP sequence in all three IP fractions and VceC peptides were detected only in the samples containing VceC or VceC$_{5\text{-}167}$ (Fig. 3C). BiP was immunoprecipitated by both VceC and VceC$_{5\text{-}167}$, indicating that the proline-rich region is not required for interaction with BiP.

Ectopically expressed VceC localizes to the ER in HeLa cells and alters its structure. The finding that VceC interacts with BiP, a protein localizing to the ER, prompted us to examine the subcellular localization of VceC in HeLa cells (Fig. 4). Confocal microscopy of cells ectopically expressing HA-VceC revealed that it colocalized with the ER marker calreticulin (Fig. 4A). Notably, the normal, fine reticular pattern of ER staining in cells expressing HA-VceC was disrupted compared to that in untransfected HeLa cells (Fig. 4A), as HA-VceC reorganized the ER into thicker tubular structures (Fig. 4A). This disruption of the ER structure required the N terminus of VceC, since truncation of the N-terminal 37 amino acids of VceC resulted in a variant that no longer targeted the ER or led to its reorganization (Fig. 4B). To ensure that the effect of HA-VceC on the ER was independent of the epitope tag, experiments were repeated with Myc-VceC and GFP-VceC fusions that were expressed in a similar manner. Similar to HA-VceC, Myc-VceC and GFP-VceC both localized to the ER of HeLa cells (GFP-VceC: Fig. 5B; Myc-VceC not shown) and also disrupted the ER structure of these cells. Expression of VceC did not lead to an overall disruption of cellular architecture, since the actin cytoskeleton appeared unchanged in cells expressing VceC (Fig. 4C).

Since *Brucella* is known to infect primarily phagocytic cells, the localization of VceC in transfected RAW264.7 mouse macrophages was determined (Fig. 4D). Similar to what was observed in HeLa cells, HA-VceC localized to the ER of RAW264.7 cells and the ER network. Taken together, these results indicate that VceC targets the ER, the subcellular compartment from which the *B. abortus* replication niche is derived.

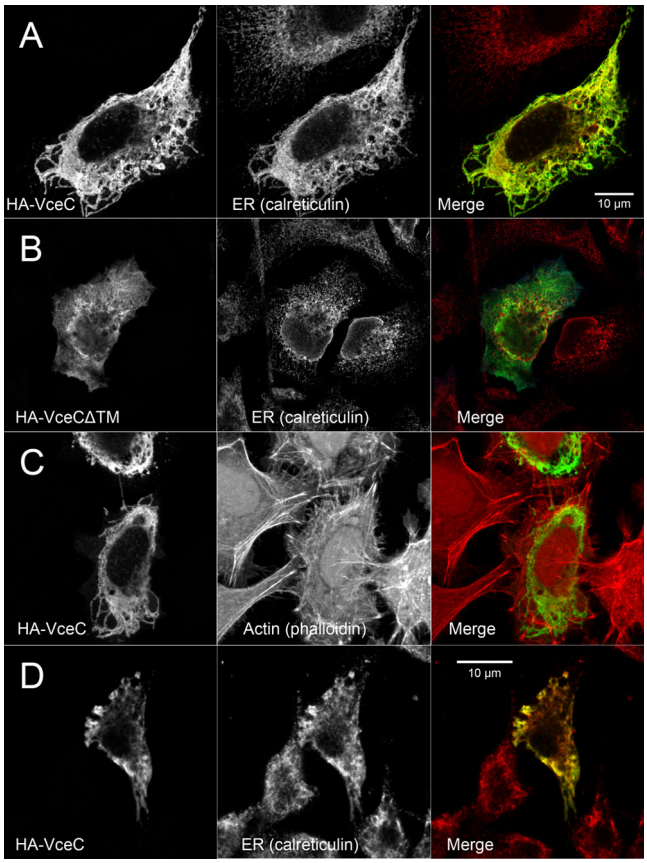

FIG 4 Localization of HA-VceC fusions in HeLa cells (A to C) and RAW264.7 macrophages (D). Transfected cells grown on coverslips were stained with anti-calreticulin antibody (red) to visualize the ER (A, B, and D) or with phalloidin (red) to visualize the actin cytoskeleton (C). HA-VceC and HA-VceC$_{38\text{-}418}$ were visualized with anti-HA antibody (green). The images shown are representative of at least three independent experiments.

VceC requires a hydrophobic domain at its N terminus for ER localization. In addition to the proline-rich region mentioned above, *B. abortus* VceC is predicted to contain a hydrophobic TM domain at its N terminus (Fig. 5A). To determine the regions of VceC required for ER localization, a series of truncated VceC proteins lacking the N-terminal TM domain (VceC$_{38\text{-}418}$), a C-terminal domain (VceC$_{5\text{-}325}$), or the central proline-rich domain (VceC$_{5\text{-}167}$) was expressed in HeLa cells (Fig. 5). Both GFP-VceC$_{5\text{-}325}$, truncated at the C terminus, and GFP-VceC$_{5\text{-}167}$, lacking both the C terminus and the proline-rich region, localized to the ER. The ER structures of HeLa cells expressing GFP-VceC$_{5\text{-}325}$ and GFP-VceC$_{5\text{-}167}$ appeared to be disrupted similarly to that of cells expressing full-length VceC, suggesting that neither the C terminus nor the proline-rich region is required for perturbation of the ER structure upon the expression of VceC (Fig. 5B). However, in contrast to full-length VceC, VceC$_{38\text{-}418}$ did not localize to the ER, but rather was distributed diffusely in the cytoplasm (Fig. 5B), suggesting that the N-terminal 37 amino acids containing the predicted TM domain are required for ER localization of VceC. VceC$_{38\text{-}418}$ also failed to colocalize with BiP (Fig. 5C), suggesting that this interaction requires the localization of VceC to the ER.

The proinflammatory response induced by VceC shares features with the ER stress response. BiP/Grp78, identified above as

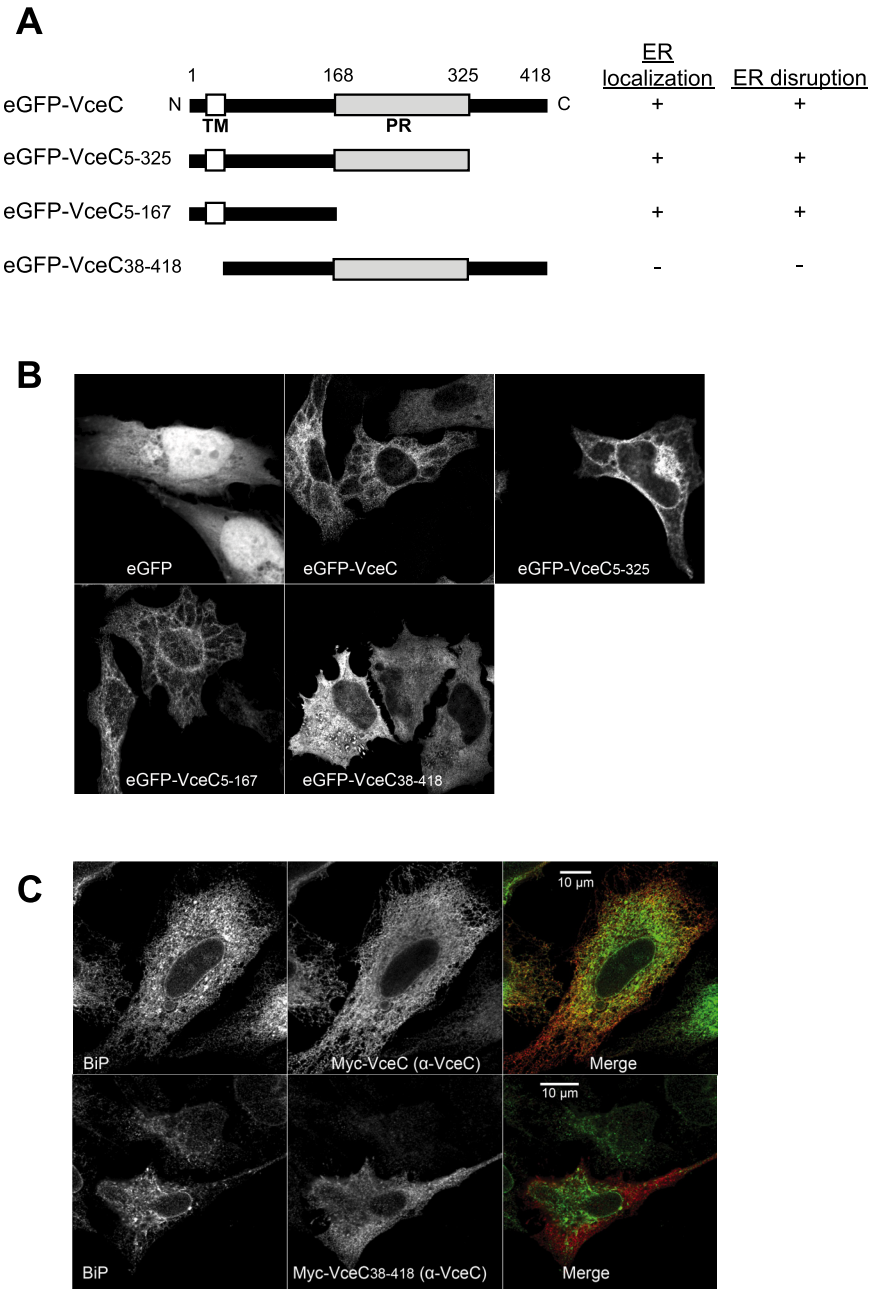

FIG 5 Localizations of GFP-VceC truncations in HeLa cells. (A) Schematic representation of *B. abortus* VceC showing the putative TM domain and the proline-rich (PR) region. Also shown are the observed localizations of the fusion proteins and their disruptive influences on the integrity of the ER. (B) Localization of the GFP-VceC fusion protein in the cytoplasm or ER of HeLa cells. Colocalization of GFP with the ER marker calreticulin was used to determine the ER localization of the GFP-VceC fusion protein. (C) Colocalization of VceC, but not $VceC_{38-418}$, with BiP. The results shown are representative images from at least three independent experiments.

an interaction partner of VceC, plays a central role in the maintenance of ER homeostasis. Under homeostatic conditions, BiP sequesters ER membrane proteins that function in the unfolded protein response (UPR), including the double-stranded-RNA-dependent protein kinase-like ER kinase (PERK), activating transcription factor 6 (ATF6), and inositol-requiring TM kinase/endonuclease 1 (IRE1α), thereby preventing their activation (reviewed in reference 39). Perturbation of the ER, for example, via accumulation of unfolded proteins, results in recruitment of BiP to the unfolded proteins, thereby releasing it from PERK, ATF6, and IRE1α, which permits the activation of these proteins by phosphorylation and initiation of the UPR.

We hypothesized that during infection, translocation of VceC into host cells, followed by VceC targeting to the ER and binding to BiP, could lead to activation of the UPR. To test this hypothesis, we infected BMDM with the *B. abortus* wild type, the *vceC* mutant (MDJ32), or the complemented *vceC* mutant and measured the induction of IL-6, the induction of the ER stress markers BiP (40) and Sec61γ (41), and the splicing of the XBP1 mRNA (27, 42). As a positive control for ER stress and UPR induction, uninfected macrophages were treated with tunicamycin (41, 43, 44). Interestingly, treatment of macrophages with tunicamycin induced IL-6 expression to an extent similar to that of infection with *B. abortus* (Fig. 6A), consistent with a possible association between the UPR and the inflammatory response induced by VceC. A feature of the UPR is upregulation of proteins that relieve ER stress, including BiP and Sec61γ, a component of the Sec61 translocon (39). Infection with *B. abortus* or treatment with tunicamycin resulted in increased levels of both *hspa5* (encoding BiP) and *sec61g* (encoding Sec61γ) transcripts (Fig. 6B and C). The increased expression of these genes was dependent on VceC, and the reduced induction observed during infection with the *vceC* mutant was restored in the complemented strain.

A second feature of ER stress is splicing of the mRNA for the transcription factor XBP1, which occurs when BiP is released from the ER-localized splicing enzyme IRE1. The splicing of XBP1 mRNA allows for its translation to form a stable protein (39). This splicing was reduced in cells infected with the *vceC* mutant and was restored in cells infected with the complemented *vceC* mutant (Fig. 6D).

To determine whether ER stress is required for sensing of VceC translocation during infection with *B. abortus*, we knocked down the expression of IRE1 in BMDM by using siRNA (Fig. 6E to G). In BMDM treated with siRNA, expression of IRE1 was reduced by 75%, on average (Fig. 6E). Further, knockdown of IRE1 in BMDM did not affect the bacterial numbers of *B. abortus* at 24 h p.i. (Fig. 6F). Knockdown of IRE1 expression resulted in a significant reduction of IL-6 secretion by BMDM infected with wild-type *B. abortus*, or treated with tunicamycin, demonstrating that in both cases, the

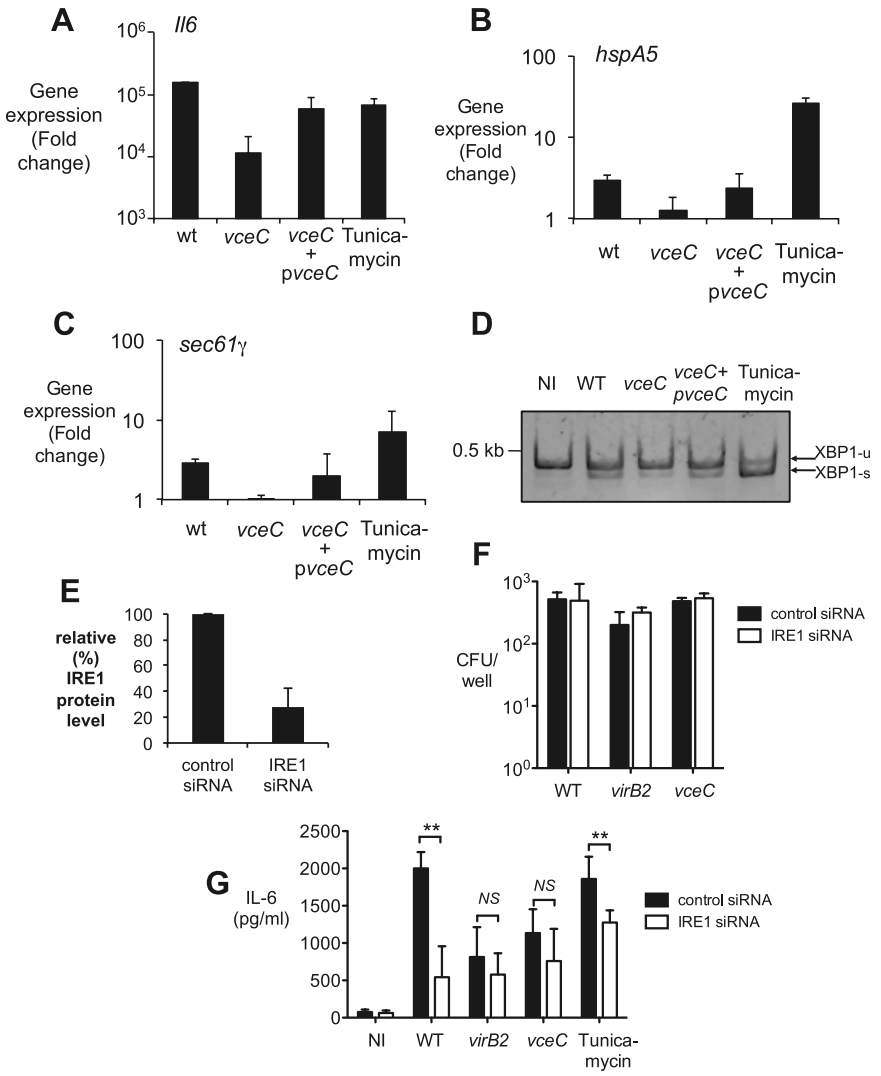

FIG 6 VceC-dependent induction of IL-6 and ER stress markers in BMDM infected with *B. abortus*. RNA was isolated from macrophages that had been infected for 24 h with wild-type (wt or WT) *B. abortus* (2308), the *vceC* mutant MDJ32, or the complemented *vceC* mutant MDJ71 or treated with 3.5 μg/ml tunicamycin. All cells were treated with 1 ng/ml IFN-γ for 24 h. (A to C) Levels of IL-6 (A), *hspA5* (BiP; B), and *sec61g* (C) mRNAs were determined by qRT-PCR. Each value shown is the *n*-fold induction over the mRNA level in uninfected macrophages. (D) Splicing of the XBP-1 transcript in BMDM infected with *B. abortus* strains or treated with tunicamycin for 24 h. An increase in spliced XBP1 mRNA (XBP1-s) was observed in macrophages infected with wild-type *B. abortus* compared to that in uninfected macrophages or macrophages infected with the *vceC* mutant (MDJ32). NI, not infected. (E to G) Knockdown of IRE1 in BMDM. (E) Quantification of IRE1 in BMDM treated with either control or IRE1-specific siRNA pools by densitometric analysis of Western blots. (F) Intracellular numbers of CFU of *B. abortus* strains treated with control or IRE1-specific siRNA pools. (G) Induction of IL-6 24 h after *B. abortus* infection of BMDM treated with IRE1-specific or control siRNA pools. The results shown are means ± standard errors of data from three independent experiments. The Student *t* test was used to analyze differences between individual sets of data. **, $P < 0.01$. ns, no significant difference.

proinflammatory signaling depended on the UPR (Fig. 6G). In contrast, IRE1 knockdown did not affect IL-6 secretion induced by the *virB2* or *vceC* mutant. These results implicate the UPR in the sensing of VceC translocation by *B. abortus* in infected macrophages.

VceC-induced NF-κB activation requires its localization to the ER. The results presented above suggest that the translocation of VceC into host cells leads to its localization to the ER, where it is sensed by an ER stress pathway that leads to the activation of NF-κB-dependent cytokines. To verify these results by using a different experimental approach and to eliminate the influence of other *Brucella* factors, we ectopically expressed HA-VceC in HEK293 cells that were transfected with an NF-κB luciferase reporter construct. While the expression of full-length HA-VceC resulted in NF-κB activation, HA-VceC$_{38-418}$, lacking the TM domain required for ER targeting (Fig. 5B), failed to activate NF-κB above the level of the empty control plasmid (Fig. 7), suggesting that ER targeting of VceC is required for its proinflammatory activity.

DISCUSSION

The ER functions in the biosynthesis, folding, and modification of both soluble and membrane proteins, as well as in the maintenance of calcium homeostasis. Perturbations of cellular physiology that disrupt these functions can lead to the accumulation of unfolded or misfolded proteins in the ER lumen, a condition known as ER stress (33). To maintain cellular homeostasis, the UPR is induced. This response involves multiple pathways that alter both transcription and translation, thereby allowing the cell to resolve ER stress by reducing the influx of new proteins into the ER (39).

Our results suggest that the T4SS-secreted protein VceC can also trigger the UPR, resulting in the induction of inflammation by *B. abortus*. A connection between ER stress and NF-κB signaling was discovered almost 20 years ago (44, 45). More recently, it has been shown that both infectious and noninfectious processes can trigger ER stress and UPR-dependent NF-κB signaling, including cleavage of BiP by the subtilase cytotoxin of enterohemorrhagic *Escherichia coli* (46) and retention of antigen in the ER of B lymphocytes (47). Our results show that the induction of this pathway by a secreted bacterial effector, VceC, might serve as a pattern of pathogenesis that induces inflammation. Interestingly, a group of *Legionella pneumophila* T4SS effectors activates NF-κB signaling by inhibiting protein synthesis in infected host cells (5). Since inhibition of translation is a downstream component of the UPR, our results suggest that different points in the same pathway can be targeted by diverse bacterial proteins.

While our results suggest that VceC-mediated induction of the UPR triggers proinflammatory responses, it is unclear whether this is dependent on the interaction between VceC and BiP. BiP

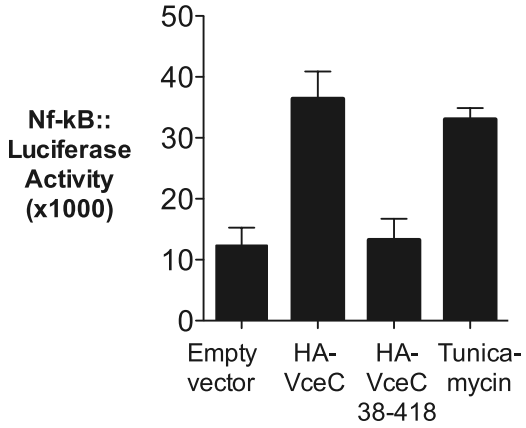

FIG 7 Activation of NF-κB by HA-VceC but not by $VceC_{38-418}$. HEK293 cells were transfected for 48 h with a vector for the expression of full-length HA-VceC or truncated HA-$VceC_{38-418}$. As a negative control, cells were transfected with an empty vector, and as a positive control for NF-κB activation, cells were transfected with an empty vector and treated with 2 μg/ml tunicamycin. The results shown are means ± standard deviations of three independent experiments.

binds to unfolded stretches of proteins, with a preference for hydrophobic domains (33). Thus, the interaction of VceC with BiP could be a result of its localization in the ER, rather than a specific mechanism for initiating the UPR. An alternate interpretation of our results is that an activity of VceC that is independent of binding to BiP may provide a stimulus that induces the UPR. One piece of evidence that suggests that the VceC-BiP interaction may be relevant for induction of the UPR is the disorganization of ER structure that was observed on the expression of VceC in HeLa cells (Fig. 4), which resembled the phenotype observed when BiP was knocked down in cells with siRNA (48). Our results do show, however, that localization of VceC to the ER was required for induction of NF-κB, as we observed no activation of this pathway by an N-terminally truncated VceC variant that failed to target the ER (Fig. 7A).

ER stress is known to elicit both apoptotic and autophagic pathways. Infection with *B. suis* and *B. melitensis* is associated with inhibition of cell death pathways (49, 50), suggesting that other signals in addition to UPR induction may be needed to induce apoptosis. *B. abortus* infection has recently been shown to induce selective autophagy of BCVs by a noncanonical pathway (23). However, deletion of *vceC* did not affect this intracellular stage of the bacterium's cycle, since a *vceC* mutant still formed aBCVs (see Fig. S2 in the supplemental material), suggesting that this protein is not essential for the induction of this novel autophagic pathway by *B. abortus* or that it may work redundantly with other, as-yet-unidentified, effectors to elicit this pathway. In contrast, both the induction of XBP-1 splicing by VceC and the dependence of the VceC-dependent inflammatory response on IRE1 suggest that the IRE1 arm of the UPR is activated by VceC (Fig. 6E to G; see Fig. S3 in the supplemental material). Interestingly, IRE1 was shown previously to be required for the intracellular replication of *B. abortus*, since IRE1 deficiency rendered *Drosophila* S2 cells or murine embryonic fibroblasts nonpermissive for *B. abortus* replication (51). It should be pointed out that unlike nonphagocytic cells, the IFN-γ-activated BMDM in our study are not highly permissive of the intracellular replication of *B. abortus*; therefore, our results do not address whether IRE1 is required for intracellular replication. However, if IRE1 is also required for the replication of *B. abortus* in macrophages, then additional *B. abortus* factors must act on IRE1 to promote intracellular replication, since inactivation of *vceC* alone did not affect the replication competence of *B. abortus* in a more permissive macrophage cell line, J774 (see Fig. S1C in the supplemental material).

The picture emerging from this and previous studies is that the UPR represents a surveillance pathway that detects both viral and bacterial intrusions into the ER and induces inflammatory responses to infection. While UPR-induced NF-κB signaling may represent a novel host surveillance pathway for bacterial effectors, *B. abortus* seems to exploit this pathway to its benefit *in vivo*, since VceC provided a modest advantage for long-term colonization of the mouse. Perhaps more importantly, T4SS-mediated inflammation leads to abortion in a mouse model (52). T4SS-mediated inflammation might thus increase the fitness of *B. abortus*, because abortion is the main route of pathogen transmission within its natural bovine animal reservoir (53).

MATERIALS AND METHODS

Bacterial strains and plasmids. For the *B. abortus* and *E. coli* strains used in this study, see Table S1 in the supplemental material. *B. abortus* 2308 was used as the wild-type strain. *Brucella* strains were cultured on tryptic soy agar (Difco/Becton, Dickinson, Sparks, MD), in tryptic soy broth (TSB) with appropriate antibiotics, or in modified E medium (26). *E. coli* strains were grown in lysogeny broth that was solidified with agar as needed. Antibiotics were used at the following concentrations for *E. coli* and *B. abortus*: carbenicillin, 100 μg/ml; kanamycin, 100 μg/ml; chloramphenicol, 30 μg/ml. *E. coli* and *B. abortus* were grown at 37°C. Experiments with *B. abortus* were performed at biosafety level 3 by following standard operating procedures reviewed and approved by Institutional Biosafety Committees, in compliance with NIH guidelines and CDC Select Agent Program regulations. DNA techniques were performed according to standard protocols.

Construction of plasmids. For the plasmids used in this study, see Table S1 in the supplemental material. For the primers used to generate recombinant constructs, see Table S2 in the supplemental material. For technical reasons, all constructs containing *vceC* lack the first 12 nucleotides from the predicted start codon and therefore, unless indicated otherwise, all recombinant VceC proteins start at amino acid 5.

Confocal microscopy. HeLa cells were seeded on 12-mm coverslips in 24-well plates at 5×10^4 cells per well. After 24 h, cells were transfected with the different constructs containing *vceC* fusions (see Table S1 in the supplemental material) using 0.5 μg of plasmid DNA at a ratio of 2 μg of DNA to 4 μl of Fugene HD (Roche). After another 24 h, cells were washed three times with phosphate-buffered saline (PBS) and fixed with 3% paraformaldehyde for 10 min at 37°C. Fixed cells were washed again twice, and NH_4Cl (50 mM) was added for 10 min. Then, coverslips were incubated for 30 min in blocking buffer (PBS with 10% horse serum and 0.1% saponin [Sigma]) and for 40 min in blocking buffer containing primary antibodies. After three washes in PBS, the coverslips were incubated for 40 min in blocking buffer containing secondary antibodies. Finally, the coverslips were washed three times in PBS and once in water and mounted on glass slides using Mowiol (Calbiochem). The primary antibodies used were mouse anti-hemagglutinin (HA) or anti-Myc (Covance), rabbit anti-calreticulin (Thermo Scientific), rabbit anti-giantin (Covance), mouse anti-BiP (BD BioScience), and rat anti-VceC (Genovac) antibodies. The secondary antibodies used were donkey anti-mouse (Alexa 488 or Alexa 647 conjugated), donkey anti-rabbit (Alexa 488 or Alexa 568 conjugated) (from Invitrogen), and Cyanin5-conjugated anti-rat (Jackson ImmunoResearch) antibodies.

IP. For IP experiments, 15 10-by-10-cm dishes containing 8×10^5 HeLa cells each were transfected with *vceA*- or *vceC*-containing vectors.

For each dish, 6 μg of plasmid DNA was added to 600 μl Dulbecco's modified Eagle's medium and 18 μl of Fugene HD transfection reagent was added. After 15 min, this mixture was added to each dish, and 40 h later, cells were scraped from the dishes and washed twice with cold PBS. The cells were lysed by adding lysis buffer (PBS, 50 mM Tris-HCl [pH 7.6], 150 mM NaCl, 0.1% [vol/vol] NP-40, 1 mM EDTA) containing phosphatase inhibitor (1:100) and protease inhibitor III (1:500) (Calbiochem). After 15 to 25 min on ice, the lysates were centrifuged at 3,000 × *g*, for 15 min at 4°C. The supernatant was then precleared by incubation with 70 μl 50% protein A agarose (Amersham) slurry for 1 h at 4°C on a rotator. The lysate was centrifuged at 1,000 × *g* for 2 min to pellet the agarose, and the supernatant was collected. To the supernatant, 7.5 μl of anti-green fluorescent protein (GFP; Invitrogen) or anti-Myc (Covance) antibody was added (0.5 μg antibody per plate) and incubated while rotating for 1 h at 4°C. Then, 70 μl protein A agarose slurry was added for 1 to 2 h. The agarose was pelleted by low-speed centrifugation. For some samples, another 5 μl of anti-GFP or anti-Myc antibody was added to the supernatant for a second round of IP similar to that described above. The agarose was washed four times with lysis buffer and then once with lysis buffer without NP-40. A 30-μl volume of hot 2× SDS sample buffer was added, and eluates of both rounds of IP were pooled together and boiled for 5 min. Some eluates (Fig. 3A) were separated by 4 to 15% SDS-PAGE. Bands were excised and sent to the Taplin Mass Spectrometry Facility (Harvard University) for analysis by microcapillary tandem mass spectrometry (MS). Other eluates (Fig. 3C) were sent to the UC Davis Genome Center Proteomics Facility for trypsin digestion and identification of peptide fragments by liquid chromatography (LC)-MS analysis.

Infection of mice. Female C57BL/6 mice were obtained from The Jackson Laboratory (Bar Harbor, ME) and used at an age of 4 to 6 weeks. For infection experiments, groups of four or five mice were inoculated intraperitoneally (i.p.) with 0.2 ml of PBS containing a 1:1 mixture of 2 × 10^5 CFU of wild-type *B. abortus* and 2 × 10^5 CFU of MDJ32 (*vceC* mutant). Infected mice were held in microisolator cages in a biosafety level 3 facility. At appropriate time points, mice were euthanized and tissue colonization levels were determined as described previously (11). All animal experiments were approved by the University of California, Davis, Institutional Laboratory Animal Care and Use Committee and were conducted in accordance with institutional guidelines.

Infection of mouse BMDM. BMDM were obtained from C57BL/6 mice (Jackson) and were differentiated from bone marrow as previously described (11). BMDM were infected with *B. abortus* 2308, the *virB2* mutant (ADH3), the *vceC* mutant (MDJ32), or the complemented *vceC* mutant (MDJ71) at a multiplicity of infection (MOI) of 300:1. Gentamicin-resistant bacteria were quantified at various time points as described previously (11).

RNA isolation and qRT-PCR. RNA was isolated from macrophages infected as described above, using Tri-reagent (Molecular Research Center). One microgram of RNA was reverse transcribed in a final volume of 50 μl to cDNA using murine leukemia virus reverse transcriptase (Applied Biosciences). For quantitative reverse transcription (qRT)-PCR, the cDNA was used combined with primer pairs for mouse beta-actin (for threshold cycle value correction), IL-6, BiP, or Sec61γ (see Table S2 in the supplemental material) and SYBR green master mix (Applied Biosciences).

XBP-1 splicing assay. Mouse BMDM were infected with *B. abortus* strains or treated with 3.5 μg/ml tunicamycin (Sigma), and RNA was isolated and reverse transcribed to cDNA as described above. To visualize the splicing of XBP-1, a protocol developed by the Ron laboratory was used (27). PCR was performed in a total volume of 50 μl containing 2 μl cDNA, primers mXBP1-F and mXBP1-R at 10 pM each, and PCR Supermix (Invitrogen) by using the following PCR program: 94°C for 4 min; 35 cycles of 10 s at 94°C, 30 s at 63°C, and 10 s at 72°C; and 72°C for 10 min. PCR products of spliced and unspliced fragments were resolved on a 5% polyacrylamide gel in Tris-borate-EDTA.

ELISA. IL-6 and TNF-α secretion by infected mouse BMDM into the medium was measured by an enzyme-linked immunosorbent assay (ELISA) from eBioscience (mouse IL-6) or BioLegend (mouse TNF-α) according to the manufacturer's protocol.

Western blotting. For detection of BiP/Grp78, the primary antibody used was a mouse anti-BiP antibody (BD Bioscience) and the secondary antibody used was a horseradish peroxidase (HRP)-conjugated goat anti-rabbit (Bio-Rad) or an HRP-conjugated goat anti-mouse (Jackson ImmunoResearch) antibody.

Knockdown of *ern*, encoding IRE1, in BMDM. Control nontargeting pool and ERN1-targeting pool small interfering RNAs (siRNA) were purchased from Dharmacon. Mouse BMDM were transfected with an Amaxa Nucleofector and an Amaxa mouse macrophage Nucleofector kit (Lonza). Cells were seeded at 4 × 10^5 per well, and 24 h later they were infected at an MOI of 300:1. At 24 h p.i., cells were washed once and samples were taken for CFU enumeration, ELISA, and Western blotting. To determine the efficiency of inositol-requiring transmembrane (TM) kinase/endonuclease 1 (IRE1) knockdown, Western blots were probed with anti-IRE1 antibodies (Cell Signaling). The results shown are averages of three independent experiments.

Luciferase assay. HEK293 cells were seeded into 48-well plates at 40% confluence. The next day, cells were transfected with 200 ng of pCMV-HA plasmid (empty or encoding *sipA*, *vceC*, or *VceC38-418*) by using Fugene HD (Promega) or treated with 2 μg/ml tunicamycin (Sigma). Cells were also transfected with 25 ng pNFkB luciferase reporter construct and 25 ng pLacZ (a *lacZ* reporter to correct for transfection efficiency). Cells were then incubated for 48 h at 37°C in 5% CO_2. Cells were washed three times in PBS and lysed by freezing at −80°C and defrosting. A 10-μl volume of the lysate was transferred into a 96-well white OptiPlate (PerkinElmer), and 50 μl of luciferase assay solution (Promega) was added shortly before luciferase bioluminescence was measured with the luciferase assay system (Promega) and a luminometer. For normalization of transfection efficiency, β-galactosidase activity (measured with an assay from Promega) was used to adjust luciferase values (28).

SUPPLEMENTAL MATERIAL

Supplemental material for this article may be found at http://mbio.asm.org/lookup/suppl/doi:10.1128/mBio.00418-12/-/DCSupplemental.

Figure S1, EPS file, 0.5 MB.
Figure S2, EPS file, 5.2 MB.
Figure S3, EPS file, 4.2 MB.
Table S1, PDF file, 0.1 MB.
Table S2, PDF file, 0.1 MB.

ACKNOWLEDGMENTS

This work was supported by PHS grants AI050553, AI097107, and AI090387 to R.M.T. and in part by the Intramural Research Program of the National Institute of Allergy and Infectious Diseases, National Institutes of Health.

We thank Rich Eigenheer of the UC Davis Genome Center Proteomics Facility for help with MS data analysis and Andreas Bäumler and Sebastian winter for critical comments on the manuscript.

REFERENCES

1. **Blander JM, Sander LE.** 2012. Beyond pattern recognition: five immune checkpoints for scaling the microbial threat. Nat. Rev. Immunol. **12**: 215–225.
2. **Broz P, Monack DM.** 2011. Molecular mechanisms of inflammasome activation during microbial infections. Immunol. Rev. **243**:174–190.
3. **Elinav E, Strowig T, Henao-Mejia J, Flavell RA.** 2011. Regulation of the antimicrobial response by NLR proteins. Immunity **34**:665–679.
4. **Chisholm ST, Coaker G, Day B, Staskawicz BJ.** 2006. Host-microbe interactions: shaping the evolution of the plant immune response. Cell **124**:803–814.
5. **Fontana MF, Banga S, Barry KC, Shen X, Tan Y, Luo ZQ, Vance RE.** 2011. Secreted bacterial effectors that inhibit host protein synthesis are critical for induction of the innate immune response to virulent Legionella

pneumophila. PLoS Pathog. **7**:e1001289. http://dx.doi.org/10.1371/journal.ppat.1001289.
6. **Vance RE, Isberg RR, Portnoy DA.** 2009. Patterns of pathogenesis: discrimination of pathogenic and nonpathogenic microbes by the innate immune system. Cell Host Microbe **6**:10–21.
7. **Barquero-Calvo E, Chaves-Olarte E, Weiss DS, Guzmán-Verri C, Chacón-Díaz C, Rucavado A, Moriyón I, Moreno E.** 2007. Brucella abortus uses a stealthy strategy to avoid activation of the innate immune system during the onset of infection. PLoS One **2**:e631. http://dx.doi.org/10.1371/journal.pone.0000631.
8. **Conde-Álvarez R, Arce-Gorvel V, Iriarte M, Manček-Keber M, Barquero-Calvo E, Palacios-Chaves L, Chacón-Díaz C, Chaves-Olarte E, Martirosyan A, von Bargen K, Grilló MJ, Jerala R, Brandenburg K, Llobet E, Bengoechea JA, Moreno E, Moriyón I, Gorvel JP.** 2012. The lipopolysaccharide core of *Brucella abortus* acts as a shield against innate immunity recognition. PLoS Pathog. **8**:e1002675. http://dx.doi.org/10.1371/journal.ppat.1002675.
9. **Lapaque N, Takeuchi O, Corrales F, Akira S, Moriyon I, Howard JC, Gorvel JP.** 2006. Differential inductions of TNF-alpha and IGTP, IIGP by structurally diverse classic and non-classic lipopolysaccharides. Cell. Microbiol. **8**:401–413.
10. **Rolán HG, Tsolis RM.** 2008. Inactivation of the type IV secretion system reduces the Th1 polarization of the immune response to *Brucella abortus* infection. Infect. Immun. **76**:3207–3213.
11. **Rolán HG, Xavier MN, Santos RL, Tsolis RM.** 2009. Natural antibody contributes to host defense against an attenuated *Brucella abortus* virB mutant. Infect. Immun. **77**:3004–3013.
12. **Roux CM, Rolán HG, Santos RL, Beremand PD, Thomas TL, Adams LG, Tsolis RM.** 2007. *Brucella* requires a functional type IV secretion system to elicit innate immune responses in mice. Cell. Microbiol. **9**:1851–1869.
13. **de Jong MF, Sun YH, den Hartigh AB, van Dijl JM, Tsolis RM.** 2008. Identification of VceA and VceC, two members of the VjbR regulon that are translocated into macrophages by the *Brucella* type IV secretion system. Mol. Microbiol. **70**:1378–1396.
14. **den Hartigh AB, Sun YH, Sondervan D, Heuvelmans N, Reinders MO, Ficht TA, Tsolis RM.** 2004. Differential requirements for VirB1 and VirB2 during *Brucella abortus* infection. Infect. Immun. **72**:5143–5149.
15. **Hong PC, Tsolis RM, Ficht TA.** 2000. Identification of genes required for chronic persistence of *Brucella abortus* in mice. Infect. Immun. **68**:4102–4107.
16. **O'Callaghan D, Cazevieille C, Allardet-Servent A, Boschiroli ML, Bourg G, Foulongne V, Frutos P, Kulakov Y, Ramuz M.** 1999. A homologue of the *Agrobacterium tumefaciens* VirB and *Bordetella pertussis* Ptl type.IV secretion systems is essential for intracellular survival of *Brucella suis*. Mol. Microbiol. **33**:1210–1220.
17. **Sieira R, Comerci DJ, Sánchez DO, Ugalde RA.** 2000. A homologue of an operon required for DNA transfer in *Agrobacterium* is required in *Brucella abortus* for virulence and intracellular multiplication. J. Bacteriol. **182**:4849–4855.
18. **Zygmunt MS, Hagius SD, Walker JV, Elzer PH.** 2006. Identification of *Brucella melitensis* 16M genes required for bacterial survival in the caprine host. Microbes Infect. **8**:2849–2854.
19. **Boschiroli ML, Ouahrani-Bettache S, Foulongne V, Michaux-Charachon S, Bourg G, Allardet-Servent A, Cazevieille C, Liautard JP, Ramuz M, O'Callaghan D.** 2002. The *Brucella suis virB* operon is induced intracellularly in macrophages. Proc. Natl. Acad. Sci. U. S. A. **99**:1544–1549.
20. **Celli J, de Chastellier C, Franchini DM, Pizarro-Cerda J, Moreno E, Gorvel JP.** 2003. *Brucella* evades macrophage killing via VirB-dependent sustained interactions with the endoplasmic reticulum. J. Exp. Med. **198**:545–556.
21. **Celli J, Salcedo SP, Gorvel JP.** 2005. *Brucella* coopts the small GTPase Sar1 for intracellular replication. Proc. Natl. Acad. Sci. U. S. A. **102**:1673–1678.
22. **Starr T, Ng TW, Wehrly TD, Knodler LA, Celli J.** 2008. *Brucella* intracellular replication requires trafficking through the late endosomal/lysosomal compartment. Traffic **9**:678–694.
23. **Starr T, Child R, Wehrly TD, Hansen B, Hwang S, López-Otin C, Virgin HW, Celli J.** 2012. Selective subversion of autophagy complexes facilitates completion of the *Brucella* intracellular cycle. Cell Host Microbe **11**:33–45.
24. **de Barsy M, Jamet A, Filopon D, Nicolas C, Laloux G, Rual JF, Muller A, Twizere JC, Nkengfac B, Vandenhaute J, Hill DE, Salcedo SP, Gorvel JP, Letesson JJ, De Bolle X.** 2011. Identification of a *Brucella* spp. secreted effector specifically interacting with human small GTPase Rab2. Cell. Microbiol. **13**:1044–1058.
25. **Marchesini MI, Herrmann CK, Salcedo SP, Gorvel JP, Comerci DJ.** 2011. In search of *Brucella abortus* type IV secretion substrates: screening and identification of four proteins translocated into host cells through VirB system. Cell. Microbiol. **13**:1261–1274.
26. **Kulakov YK, Guigue-Talet PG, Ramuz MR, O'Callaghan D.** 1997. Response of *Brucella suis* 1330 and *B. canis* RM6/66 to growth at acid pH and induction of an adaptive acid tolerance response. Res. Microbiol. **148**:145–151.
27. **Calfon M, Zeng H, Urano F, Till JH, Hubbard SR, Harding HP, Clark SG, Ron D.** 2002. IRE1 couples endoplasmic reticulum load to secretory capacity by processing the XBP-1 mRNA. Nature **415**:92–96.
28. **Keestra AM, de Zoete MR, Bouwman LI, van Putten JP.** 2010. Chicken TLR21 is an innate CpG DNA receptor distinct from mammalian TLR9. J. Immunol. **185**:460–467.
29. **den Hartigh AB, Rolan HG, de Jong MF, Tsolis RM.** 2008. VirB3-VirB6 and VirB8-VirB11, but not VirB7, are essential for mediating persistence *Brucella* in the reticuloendothelial system. J. Bacteriol. **190**:4427–4436.
30. **Vitry MA, De Trez C, Goriely S, Dumoutier L, Akira S, Ryffel B, Carlier Y, Letesson JJ, Muraille E.** 2012. Crucial role of gamma interferon-producing $CD4^+$ Th1 cells but dispensable function of $CD8^+$ T cell, B cell, Th2, and Th17 responses in the control of *Brucella melitensis* infection in mice. Infect. Immun. **80**:4271–4280.
31. **Rolán HG, Tsolis RM.** 2007. Mice lacking components of adaptive immunity show increased *Brucella abortus virB* mutant colonization. Infect. Immun. **75**:2965–2973.
32. **Dudek J, Benedix J, Cappel S, Greiner M, Jalal C, Müller L, Zimmermann R.** 2009. Functions and pathologies of BiP and its interaction partners. Cell. Mol. Life Sci. **66**:1556–1569.
33. **Haas IG.** 1994. BiP (GRP78), an essential hsp70 resident protein in the endoplasmic reticulum. Experientia **50**:1012–1020.
34. **Haas IG, Wabl M.** 1983. Immunoglobulin heavy chain binding protein. Nature **306**:387–389.
35. **Munro S, Pelham HR.** 1986. An Hsp70-like protein in the ER: identity with the 78 kd glucose-regulated protein and immunoglobulin heavy chain binding protein. Cell **46**:291–300.
36. **Campellone KG, Robbins D, Leong JM.** 2004. EspFU is a translocated EHEC effector that interacts with Tir and N-WASP and promotes Nck-independent actin assembly. Dev. Cell **7**:217–228.
37. **Kay BK, Williamson MP, Sudol M.** 2000. The importance of being proline: the interaction of proline-rich motifs in signaling proteins with their cognate domains. FASEB J. **14**:231–241.
38. **Niebuhr K, Ebel F, Frank R, Reinhard M, Domann E, Carl UD, Walter U, Gertler FB, Wehland J, Chakraborty T.** 1997. A novel proline-rich motif present in ActA of Listeria monocytogenes and cytoskeletal proteins is the ligand for the EVH1 domain, a protein module present in the Ena/VASP family. EMBO J. **16**:5433–5444.
39. **Todd DJ, Lee AH, Glimcher LH.** 2008. The endoplasmic reticulum stress response in immunity and autoimmunity. Nat. Rev. Immunol. **8**:663–674.
40. **Kozutsumi Y, Segal M, Normington K, Gething MJ, Sambrook J.** 1988. The presence of malfolded proteins in the endoplasmic reticulum signals the induction of glucose-regulated proteins. Nature **332**:462–464.
41. **Bull VH, Thiede B.** 2012. Proteome analysis of tunicamycin-induced ER stress. Electrophoresis **33**:1814–1823.
42. **Yoshida H, Matsui T, Yamamoto A, Okada T, Mori K.** 2001. XBP1 mRNA is induced by ATF6 and spliced by IRE1 in response to ER stress to produce a highly active transcription factor. Cell **107**:881–891.
43. **Duksin D, Mahoney WC.** 1982. Relationship of the structure and biological activity of the natural homologues of tunicamycin. J. Biol. Chem. **257**:3105–3109.
44. **Pahl HL, Baeuerle PA.** 1995. A novel signal transduction pathway from the endoplasmic reticulum to the nucleus is mediated by transcription factor NF-kappa B. EMBO J. **14**:2580–2588.
45. **Pahl HL, Baeuerle PA.** 1995. Expression of influenza virus hemagglutinin activates transcription factor NF-kappa B. J. Virol. **69**:1480–1484.
46. **Yamazaki H, Hiramatsu N, Hayakawa K, Tagawa Y, Okamura M, Ogata R, Huang T, Nakajima S, Yao J, Paton AW, Paton JC, Kitamura M.** 2009. Activation of the Akt-NF-kappaB pathway by subtilase cytotoxin

through the ATF6 branch of the unfolded protein response. J. Immunol. **183**:1480–1487.
47. **Wheeler MC, Rizzi M, Sasik R, Almanza G, Hardiman G, Zanetti M.** 2008. KDEL-retained antigen in B lymphocytes induces a proinflammatory response: a possible role for endoplasmic reticulum stress in adaptive T cell immunity. J. Immunol. **181**:256–264.
48. **Li J, Ni M, Lee B, Barron E, Hinton DR, Lee AS.** 2008. The unfolded protein response regulator GRP78/BiP is required for endoplasmic reticulum integrity and stress-induced autophagy in mammalian cells. Cell Death Differ. **15**:1460–1471.
49. **Gross A, Terraza A, Ouahrani-Bettache S, Liautard JP, Dornand J.** 2000. In vitro *Brucella suis* infection prevents the programmed cell death of human monocytic cells. Infect. Immun. **68**:342–351.
50. **He Y, Reichow S, Ramamoorthy S, Ding X, Lathigra R, Craig JC, Sobral BW, Schurig GG, Sriranganathan N, Boyle SM.** 2006. Brucella melitensis triggers time-dependent modulation of apoptosis and down-regulation of mitochondrion-associated gene expression in mouse macrophages. Infect. Immun. **74**:5035–5046.
51. **Qin QM, Pei J, Ancona V, Shaw BD, Ficht TA, de Figueiredo P.** 2008. RNAi screen of endoplasmic reticulum-associated host factors reveals a role for IRE1alpha in supporting *Brucella* replication. PLoS Pathog. **4**:e1000110. http://dx.doi.org/10.1371/journal.ppat.1000110.
52. **Kim S, Lee DS, Watanabe K, Furuoka H, Suzuki H, Watarai M.** 2005. Interferon-gamma promotes abortion due to *Brucella* infection in pregnant mice. BMC Microbiol. **5**:22. http://dx.doi.org/10.1186/1471-2180-5-22.
53. **Samartino LE, Enright FM.** 1993. Pathogenesis of abortion of bovine brucellosis. Comp. Immunol. Microbiol. Infect. Dis. **16**:95–101.